

The Marchenko method for evanescent waves

Kees Wapenaar

*Department of Geoscience and Engineering, Delft University of Technology, P.O. Box 5048, 2600 GA Delft, the Netherlands.
 E-mail: c.p.a.wapenaar@tudelft.nl*

Accepted 2020 August 1. Received 2020 July 31; in original form 2020 June 23

SUMMARY

With the Marchenko method, Green's functions in the subsurface can be retrieved from seismic reflection data at the surface. State-of-the-art Marchenko methods work well for propagating waves but break down for evanescent waves. This paper discusses a first step towards extending the Marchenko method for evanescent waves and analyses its possibilities and limitations. In theory both the downward and upward decaying components can be retrieved. The retrieval of the upward decaying component appears to be very sensitive to model errors, but the downward decaying component, including multiple reflections, can be retrieved in a reasonably stable and accurate way. The reported research opens the way to develop new Marchenko methods that can handle refracted waves in wide-angle reflection data.

Key words: Controlled source seismology; Seismic interferometry; Wave scattering and diffraction.

1 INTRODUCTION

Building on the single-sided autofocusing method of Rose (2002), Brogini & Snieder (2012) proposed a data-driven method to retrieve the Green's function inside a layered medium from the seismic reflection response at the surface. This method, which is based on the Marchenko equation, has been extended for laterally varying media and used for imaging the subsurface without artefacts related to internal multiple reflections (Wapenaar *et al.* 2014; Ravasi *et al.* 2016; Staring *et al.* 2018). Current Marchenko methods only handle propagating waves, which for most practical applications is acceptable. However, in reflection experiments with large horizontal offsets, which may include refracted arrivals, evanescent waves play a significant role. This paper discusses a first step towards extending the Marchenko method for evanescent waves and analyses its possibilities and limitations.

2 PROPAGATION INVARIANTS

We review propagation invariants for a horizontally layered lossless acoustic medium, which will be used for the derivation of representations for the Marchenko method in the next section. The propagation velocity $c(z)$ and mass density $\rho(z)$ are piecewise continuous functions of the depth coordinate z . In this medium, we consider a 2-D space- and time-dependent acoustic wave field, characterized by $p(x, z, t)$ and $v_z(x, z, t)$, where p is the acoustic pressure, v_z the vertical component of the particle velocity, x the horizontal coordinate and t the time. We define the temporal and spatial Fourier transform of $p(x, z, t)$ as

$$\tilde{p}(s_x, z, \omega) = \int_{-\infty}^{\infty} \int_{-\infty}^{\infty} p(x, z, t) \exp\{i\omega(t - s_x x)\} dt dx, \quad (1)$$

where i is the imaginary unit, ω the angular frequency and s_x the horizontal slowness. A similar definition holds for $\tilde{v}_z(s_x, z, \omega)$. Throughout this paper ω is taken positive or zero. Since we use slowness s_x (instead of wavenumber $k_x = \omega s_x$) as the spatial Fourier variable in $\tilde{p}(s_x, z, \omega)$, the inverse temporal Fourier transform is defined per s_x -value as

$$p(s_x, z, \tau) = \frac{1}{\pi} \Re \int_0^{\infty} \tilde{p}(s_x, z, \omega) \exp(-i\omega\tau) d\omega. \quad (2)$$

Here \Re denotes the real part and τ is the so-called intercept time (Stoffa 1989). For $\tilde{p}(s_x, z, \omega)$ as well as $p(s_x, z, \tau)$, the wave field is propagating when $|s_x| \leq 1/c(z)$ and evanescent when $|s_x| > 1/c(z)$. For propagating waves, the local propagation angle $\alpha(z)$ follows from $s_x = \sin \alpha(z)/c(z)$. Everything that follows also holds for 3-D cylindrically symmetric wave fields when the spatial Fourier transform is replaced by a Hankel transform and the horizontal slowness s_x by the radial slowness s_r .

We consider two independent acoustic states, indicated by subscripts A and B . The following combinations of wave fields in states A and B ,

$$\tilde{p}_A \tilde{v}_{z,B} - \tilde{v}_{z,A} \tilde{p}_B \quad (3)$$

and

$$\tilde{p}_A^* \tilde{v}_{z,B} + \tilde{v}_{z,A}^* \tilde{p}_B \quad (4)$$

(with the asterisk denoting complex conjugation), are propagation invariants. This means that for fixed s_x and ω these quantities are independent of the depth coordinate z in any source-free region (Kennett *et al.* 1978). A special case is obtained when we take states A and B identical: dropping the subscripts A and B in eq. (4) and multiplying by a factor 1/4, this yields the power-flux density

in the z -direction, that is,

$$j = \frac{1}{4} \{ \tilde{p}^* \tilde{v}_z + \tilde{v}_z^* \tilde{p} \}. \quad (5)$$

Next, we introduce pressure-normalized downgoing and upgoing fields \tilde{p}^+ and \tilde{p}^- , respectively, and relate these to the total fields \tilde{p} and \tilde{v}_z , via

$$\tilde{p} = \tilde{p}^+ + \tilde{p}^-, \quad (6)$$

$$\tilde{v}_z = \frac{s_z}{\rho} (\tilde{p}^+ - \tilde{p}^-). \quad (7)$$

Here $s_z(z)$ is the vertical slowness. For propagating waves it is positive real-valued or zero, according to

$$s_z = +\sqrt{1/c^2 - s_x^2}, \quad \text{for } s_x^2 \leq 1/c^2(z), \quad (8)$$

whereas for evanescent waves it is positive imaginary-valued, that is,

$$s_z = +i\sqrt{s_x^2 - 1/c^2}, \quad \text{for } s_x^2 > 1/c^2(z). \quad (9)$$

For evanescent waves, \tilde{p}^+ and \tilde{p}^- are downward and upward decaying (i.e. decaying in the $+z$ and $-z$ direction), respectively. Substitution of eqs (6) and (7) into eqs (3) and (4) yields two additional propagation invariants (Ursin 1983; Wapenaar *et al.* 1989)

$$-\frac{2s_z}{\rho} (\tilde{p}_A^+ \tilde{p}_B^- - \tilde{p}_A^- \tilde{p}_B^+) \quad (10)$$

and

$$\frac{2\Re(s_z)}{\rho} ((\tilde{p}_A^+)^* \tilde{p}_B^+ - (\tilde{p}_A^-)^* \tilde{p}_B^-) - \frac{2i\Im(s_z)}{\rho} ((\tilde{p}_A^+)^* \tilde{p}_B^- - (\tilde{p}_A^-)^* \tilde{p}_B^+), \quad (11)$$

respectively, where \Im denotes the imaginary part. The second propagation invariant consists of two terms, of which only the first term is non-zero for propagating waves, whereas for evanescent waves only the second term is non-zero. This second term was neglected in previous derivations of the Marchenko method. In a layered medium, where tunnelling of evanescent waves occurs in thin high-velocity layers, the propagation invariant of eq. (11) switches back and forth between the first and the second term, but its value is the same in each layer. Finally, for the special case that states A and B are identical we obtain for the power-flux density

$$j = \frac{\Re(s_z)}{2\rho} (|\tilde{p}^+|^2 - |\tilde{p}^-|^2) + \frac{\Im(s_z)}{\rho} \Im((\tilde{p}^+)^* \tilde{p}^-). \quad (12)$$

The first term quantifies the power-flux density of propagating waves and the second term that of tunnelling evanescent waves in high-velocity layers.

3 REPRESENTATIONS FOR THE MARCHENKO METHOD

We use the propagation invariants of eqs (10) and (11) to derive representations for the Marchenko method, analogous to Slob *et al.* (2014) and Wapenaar *et al.* (2014), but extended for evanescent waves. We consider a layered source-free lossless medium for $z \geq z_0$. For state B we consider a Green's function $\tilde{G} = \tilde{G}^+ + \tilde{G}^-$, with its source (scaled with $-i\omega\rho$) just above z_0 . At z_0 , the downgoing Green's function \tilde{G}^+ equals $\rho(z_0)/2s_z(s_x, z_0)$ (Aki & Richards 1980; Fokkema & van den Berg 1993). The wave fields \tilde{p}_B^+ and \tilde{p}_B^- at z_0 (just below the source) and at z_F (an arbitrarily chosen focal depth inside the medium) are given in Table 1. Note that $\tilde{R}^U(s_x, z_0, \omega)$ denotes the reflection response ‘‘from above’’ of the

layered medium. For state A we introduce a focusing function $\tilde{f}_1 = \tilde{f}_1^+ + \tilde{f}_1^-$ in a truncated medium, which is identical to the actual medium above the focal depth z_F and homogeneous below it. The downgoing focusing function $\tilde{f}_1^+(s_x, z, z_F, \omega)$ is defined such that, when emitted from $z = z_0$ into the medium, it focuses at z_F . Its propagation to the focal depth z_F is described by $\tilde{T}^+(s_x, z_F, z_0, \omega) \tilde{f}_1^+(s_x, z_0, z_F, \omega) = \tilde{f}_1^+(s_x, z_F, z_F, \omega)$, where $\tilde{T}^+(s_x, z_F, z_0, \omega)$ is the downgoing transmission response of the truncated medium and $\tilde{f}_1^+(s_x, z_F, z_F, \omega)$ is the focused field at z_F . We could define $\tilde{f}_1^+(s_x, z_F, z_F, \omega) = 1$, where 1 is the Fourier transform of a temporal delta function. However, in analogy with the downgoing Green's function at z_0 , we define $\tilde{f}_1^+(s_x, z_F, z_F, \omega) = \rho(z_F)/2s_z(s_x, z_F)$, see Table 1. We thus obtain

$$\tilde{f}_1^+(s_x, z_0, z_F, \omega) = \frac{\rho(z_F)}{2s_z(s_x, z_F)} \frac{1}{\tilde{T}^+(s_x, z_F, z_0, \omega)}. \quad (13)$$

Hence, the downgoing focusing function $\tilde{f}_1^+(s_x, z_0, z_F, \omega)$ is defined as a scaled inverse of the transmission response of the truncated medium. The upgoing focusing function $\tilde{f}_1^-(s_x, z_0, z_F, \omega)$ is the reflection response of the truncated medium to $\tilde{f}_1^+(s_x, z_0, z_F, \omega)$. Since the half-space below the truncated medium is homogeneous, we have $\tilde{f}_1^-(s_x, z_F, z_F, \omega) = 0$.

The propagation invariants are now used to relate the quantities in Table 1 at z_0 to those at z_F . From propagation invariant (10) we obtain (for propagating and evanescent waves)

$$\begin{aligned} \tilde{G}^-(s_x, z_F, z_0, \omega) + \tilde{f}_1^-(s_x, z_0, z_F, \omega) \\ = \tilde{R}^U(s_x, z_0, \omega) \tilde{f}_1^+(s_x, z_0, z_F, \omega), \end{aligned} \quad (14)$$

or, using the inverse Fourier transform defined in eq. (2),

$$\begin{aligned} G^-(s_x, z_F, z_0, \tau) + \tilde{f}_1^-(s_x, z_0, z_F, \tau) \\ = \int_{-\infty}^{\tau} R^U(s_x, z_0, \tau - \tau') \tilde{f}_1^+(s_x, z_0, z_F, \tau') d\tau'. \end{aligned} \quad (15)$$

Next we use propagation invariant (11). First we consider propagating waves at z_0 and z_F . For this situation we only use the first term of this propagation invariant. Substituting the quantities of Table 1 and applying the inverse Fourier transform of eq. (2), we obtain

$$\begin{aligned} G^+(s_x, z_F, z_0, \tau) - \tilde{f}_1^+(s_x, z_0, z_F, -\tau) \\ = - \int_{-\infty}^{\tau} R^U(s_x, z_0, \tau - \tau') \tilde{f}_1^-(s_x, z_0, z_F, -\tau') d\tau'. \end{aligned} \quad (16)$$

Next, we consider propagating waves at z_0 and evanescent waves at z_F . Equating the first term of propagation invariant (11) at z_0 to the second term at z_F , we obtain for the quantities of Table 1 (after an inverse Fourier transform)

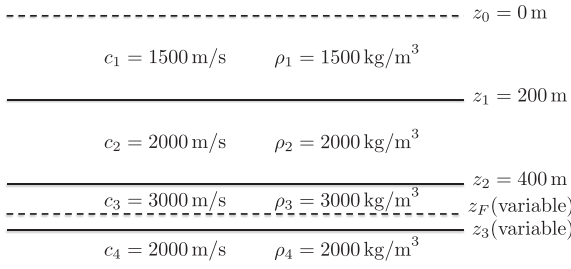
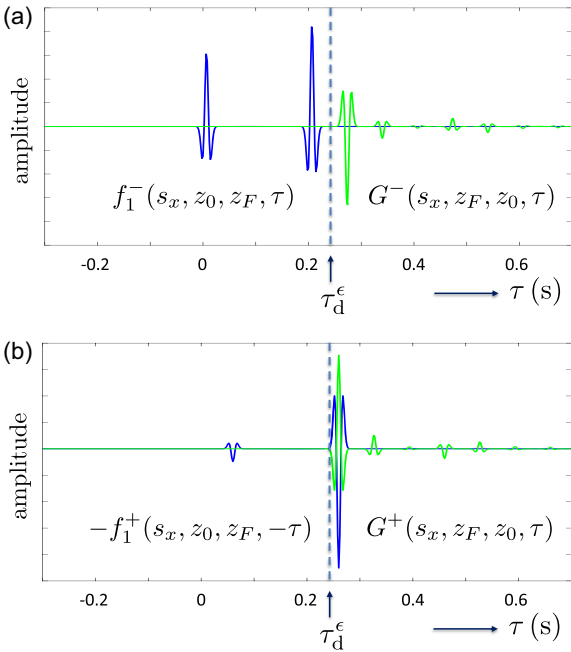
$$\begin{aligned} G^-(s_x, z_F, z_0, \tau) - \tilde{f}_1^+(s_x, z_0, z_F, -\tau) \\ = - \int_{-\infty}^{\tau} R^U(s_x, z_0, \tau - \tau') \tilde{f}_1^-(s_x, z_0, z_F, -\tau') d\tau'. \end{aligned} \quad (17)$$

Eqs (15) and (16) were already known but eq. (17) is new. It expresses the upward decaying part of the Green's function at z_F in terms of the reflection response at the surface and focusing functions. Note that two more relations can be derived for evanescent fields at z_0 , but these will not be discussed here.

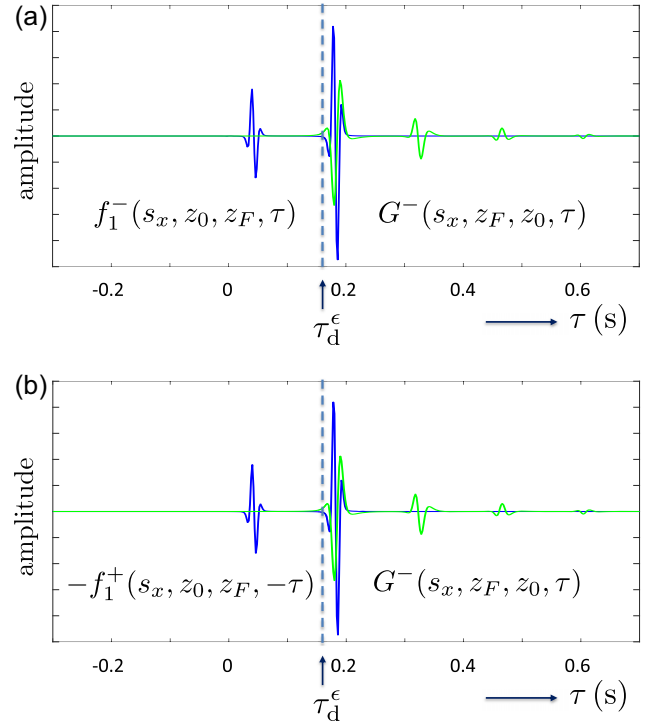
We discuss some aspects of eqs (15)–(17). Consider the medium of Fig. 1, with $z_F = 480$ m and $z_3 = 500$ m. Fig. 2 shows the functions in the left-hand sides of eqs (15) and (16), convolved with a seismic wavelet (central frequency 50 Hz), for $s_x = 0$ s m⁻¹, hence, for propagating waves at z_0 and z_F . The focusing functions are shown in blue and the Green's functions in green. The traveltimes of the

Table 1. Quantities to derive representations (15)–(17).

	$\tilde{p}_A^+(s_x, z, \omega)$	$\tilde{p}_A^-(s_x, z, \omega)$	$\tilde{p}_B^+(s_x, z, \omega)$	$\tilde{p}_B^-(s_x, z, \omega)$
$z = z_0$	$\tilde{f}_1^+(s_x, z_0, z_F, \omega)$	$\tilde{f}_1^-(s_x, z_0, z_F, \omega)$	$\frac{\rho(z_0)}{2s_z(s_x, z_0)}$	$\frac{\rho(z_0)\tilde{R}^\cup(s_x, z_0, \omega)}{2s_z(s_x, z_0)}$
$z = z_F$	$\frac{\rho(z_F)}{2s_z(s_x, z_F)}$	0	$\tilde{G}^+(s_x, z_F, z_0, \omega)$	$\tilde{G}^-(s_x, z_F, z_0, \omega)$


Figure 1. Horizontally layered lossless acoustic medium.

Figure 2. Functions in the left-hand sides of (a) eq. (15) and (b) eq. (16), for propagating waves at z_0 and z_F .

direct arrival of the downgoing Green's function in Fig. 2(b) is τ_d . The onset of this direct arrival is indicated by $\tau_d^\epsilon = \tau_d - \epsilon$, where ϵ is half the duration of the wavelet. Note that in Figs 2(a) and (b), τ_d^ϵ separates the focusing functions (at $\tau < \tau_d^\epsilon$) from the Green's functions (at $\tau > \tau_d^\epsilon$), except for the coinciding direct arrivals in Fig. 2(b) (eq. 16). This separation is an essential requirement for the standard Marchenko method. Next, consider again the medium of Fig. 1, this time with $z_F = 420$ m and $z_3 = 430$ m. The third layer between z_2 and z_3 is now a thin layer. Fig. 3 shows the functions in the left-hand sides of eqs (15) and (17) for $s_x = 1/2800$ s m⁻¹, hence, for propagating waves at z_0 and evanescent waves at z_F . Note that for this situation there appear to be coinciding arrivals in both equations, hence, the aforementioned requirement for the standard Marchenko method is not fulfilled. The mentioned arrivals will remain coincident even when the focal depth z_F is varied within the thin layer, since for evanescent waves the travelttime does not vary with depth.


Figure 3. Functions in the left-hand sides of (a) eq. (15) and (b) eq. (17), for propagating waves at z_0 and evanescent waves at z_F . In this display the amplitudes of the focusing functions are scaled by a factor 1/8.

To resolve this issue, we derive a relation between f_1^+ and f_1^- . To this end, we first introduce focusing functions f_2^+ and f_2^- (Wapenaar *et al.* 2014). The upgoing focusing function $\tilde{f}_2^-(s_x, z, z_0, \omega)$ is defined such that, when emitted from $z = z_F$ into the truncated medium, it focuses at z_0 . In Table 1 we replace the quantities in state *B* by $\tilde{p}_B^+(s_x, z_F, \omega) = \tilde{f}_2^+(s_x, z_F, z_0, \omega)$, $\tilde{p}_B^-(s_x, z_0, \omega) = \tilde{f}_2^-(s_x, z_0, z_0, \omega) = \rho(z_0)/2s_z(s_x, z_0)$ and $\tilde{p}_B^+(s_x, z_0, \omega) = 0$. State *A* remains unchanged. From propagation invariant (10) we obtain (after an inverse Fourier transform)

$$f_1^+(s_x, z_0, z_F, \tau) = f_2^-(s_x, z_F, z_0, \tau). \quad (18)$$

From propagation invariant (11) we obtain for propagating waves at z_0 and evanescent waves at z_F

$$-f_1^-(s_x, z_0, z_F, -\tau) = f_2^-(s_x, z_F, z_0, \tau). \quad (19)$$

Combining these two equations yields

$$f_1^-(s_x, z_0, z_F, \tau) = -f_1^+(s_x, z_0, z_F, -\tau). \quad (20)$$

Using this in either eqs (15) or (17) gives

$$\begin{aligned} G^-(s_x, z_F, z_0, \tau) - f_1^+(s_x, z_0, z_F, -\tau) \\ = \int_{-\infty}^{\tau} R^\cup(s_x, z_0, \tau - \tau') f_1^+(s_x, z_0, z_F, \tau') d\tau'. \end{aligned} \quad (21)$$

Hence, for the situation of propagating waves at z_0 and evanescent waves at z_F , we have reduced the system of eqs (15) and (17) to

the single eq. (21). Since coincident arrivals occur now only in one equation (illustrated by Fig. 3b), we have achieved a situation which can be solved with a modified Marchenko method (to be discussed in the next section). This yields $f_1^+(s_x, z_0, z_F, \tau)$, $G^-(s_x, z_F, z_0, \tau)$ and (via eq. 20) $f_1^-(s_x, z_0, z_F, \tau)$.

We still need a representation for $G^+(s_x, z_F, z_0, \tau)$, which we derive as follows. In the original Table 1, we replace the quantities in state *A* by $\tilde{p}_A^-(s_x, z_F, \omega) = 1$, $\tilde{p}_A^+(s_x, z_F, \omega) = \tilde{R}^\cap(s_x, z_F, \omega)$, $\tilde{p}_A^-(s_x, z_0, \omega) = \tilde{T}^-(s_x, z_0, z_F, \omega)$ and $\tilde{p}_A^+(s_x, z_0, \omega) = 0$. Here $\tilde{R}^\cap(s_x, z_F, \omega)$ denotes the reflection response ‘from below’ of the truncated medium and $\tilde{T}^-(s_x, z_0, z_F, \omega)$ its upgoing transmission response. State *B* remains unchanged. From propagation invariant (10) we obtain, after an inverse Fourier transform, using $s_2(s_x, z_0)\rho(z_F)T^-(s_x, z_0, z_F, \tau) = s_2(s_x, z_F)\rho(z_0)T^+(s_x, z_F, z_0, \tau)$ (Wapenaar 1998),

$$G^+(s_x, z_F, z_0, \tau) = \frac{\rho(z_0)T^+(s_x, z_F, z_0, \tau)}{2s_2(s_x, z_0)} + \int_{-\infty}^{\tau} R^\cap(s_x, z_F, \tau - \tau') \times G^-(s_x, z_F, z_0, \tau')d\tau'. \quad (22)$$

According to eq. (13), $T^+(s_x, z_F, z_0, \tau)$ can be obtained from $f_1^+(s_x, z_0, z_F, \tau)$. We propose to approximate the unknown $R^\cap(s_x, z_F, \tau)$ by its first reflection, coming from the deepest interface above z_F . Since this is a reflection response for evanescent waves, its amplitude is small and its arrival time is zero, hence it does not require an accurate model.

4 MARCHENKO METHOD FOR EVANESCENT WAVES

We use eq. (21) as the basis for deriving a modified Marchenko method for the situation of propagating waves at z_0 and evanescent waves at z_F . Our first aim is to suppress the Green’s function G^- from this equation, so that we are left with an equation for the focusing function f_1^+ . We write this focusing function as

$$f_1^+(s_x, z_0, z_F, \tau) = f_{1,d}^+(s_x, z_0, z_F, \tau) + M^+(s_x, z_0, z_F, \tau), \quad (23)$$

where $f_{1,d}^+$ is the direct arrival and M^+ the coda. The time-reversed direct arrival is coincident with the direct arrival of G^- , whereas the time-reversed coda is separated in time from G^- , see Fig. 3(b) for an example. We define a window function $w(\tau) = \theta(\tau_d^\epsilon - \tau)$, where $\theta(\tau)$ is the Heaviside step function. Applying this window to both sides of eq. (21) gives

$$M^+(s_x, z_0, z_F, -\tau) = -w(\tau) \int_{-\infty}^{\tau} R^\cup(s_x, z_0, \tau - \tau') \times f_1^+(s_x, z_0, z_F, \tau')d\tau'. \quad (24)$$

This equation, with M^+ replaced by $f_1^+ - f_{1,d}^+$, can be solved with the following iterative scheme

$$f_{1,k+1}^+(s_x, z_0, z_F, -\tau) = f_{1,d}^+(s_x, z_0, z_F, -\tau) - w(\tau) \times \int_{-\infty}^{\tau} R^\cup(s_x, z_0, \tau - \tau') \times f_{1,k}^+(s_x, z_0, z_F, \tau')d\tau'. \quad (25)$$

The scheme starts with $f_{1,1}^+ = f_{1,d}^+$, where $f_{1,d}^+$ is obtained by inverting the direct arrival of the transmission response of the truncated medium, analogous to eq. (13). Because of the evanescent behaviour of the transmission response, the amplitude of $f_{1,d}^+$ grows rapidly

with increasing z_F , hence, $f_{1,d}^+$ is stable only for a finite depth interval in the layer where waves are evanescent.

Hence, when the reflection response R^\cup and the direct arrival of the focusing function, $f_{1,d}^+$, are known, the iterative scheme of eq. (25) yields f_1^+ . Subsequently, eqs (22) and (21) yield $G^+(s_x, z_F, z_0, \tau)$ and $G^-(s_x, z_F, z_0, \tau)$. In these retrieved Green’s functions, z_F indicates the position of a virtual receiver which observes downward and upward decaying evanescent waves, respectively (or, via reciprocity, a virtual source which emits upward and downward decaying evanescent waves).

We illustrate this for the medium of Fig. 1, again with $z_F = 420$ m and $z_3 = 430$ m. Fig. 4(a) shows the reflection response $R^\cup(s_x, z_0, \tau)$ for $s_x = 1/2800$ s m⁻¹. The direct focusing function $f_{1,d}^+(s_x, z_0, z_F, \tau)$, shown in Fig. 4(b), has been derived from the direct transmission response, modelled for the moment in the exact truncated medium. After three iterations, we obtain the results shown in Figs 4(c), (d) and (e) (actually, for this simple medium the method converges already after one iteration and remains stable even after 100 iterations). The results (shown again in blue and green) overlay the directly modelled exact results (shown in red). Note that the match is excellent (both for the primary and the multiples) despite the simple approximation used for R^\cap , described below eq. (22).

Numerical experiments, using erroneous velocities for modelling the direct transmission response, reveal that the method is stable with respect to small velocity errors for estimating f_1^+ , but unstable for estimating G^- (unlike the Marchenko method for propagating waves). This means that in practical applications G^- cannot be obtained and that the representation for G^+ (eq. 22) should be approximated by the first term. This obviates the need for estimating $R^\cap(s_x, z_F, \tau)$. Fig. 5(a) shows G^+ obtained from the first term in eq. (22). Apart from some amplitude errors, the result is still accurate. Fig. 5(b) shows again G^+ , but this time after modelling the direct transmission response in an erroneous truncated medium, with velocities $\bar{c}_1 = 1450$, $\bar{c}_2 = 2050$ and $\bar{c}_3 = 3030$ m s⁻¹. We observe similar amplitude errors as in Fig. 5(a) and in addition some traveltimes errors caused by the wrong velocities. Nevertheless, primary and multiples are still clearly discernible and no scattering artefacts related to wrong velocities have come up. Next we replace the thin layer by a homogeneous half-space $z > z_2$ (with $c_3 = 3000$ m s⁻¹). Fig. 5(c) shows the retrieved G^+ (using the same erroneous truncated medium). Since in this situation G^- is absent at z_F , the first term in eq. (22) suffices to retrieve G^+ . This explains why the amplitudes in Fig. 5(c) are again very accurate. Finally, we apply the Marchenko method for many focal depths (using the standard method for $z_0 < z_F \leq z_2$ and the new method for evanescent waves for $z_F > z_2$). The result is shown in Fig. 6. Below the interface at $z_2 = 400$ m we clearly observe the retrieved downward decaying Green’s function, including multiple reflections related to the overlying medium. For $z_F > 480$ m the method becomes unstable and the results have been set to zero.

5 CONCLUDING REMARKS

The analysis in this paper shows that, at least in principle, the evanescent field of the Green’s function for a virtual receiver (or via reciprocity a virtual source) inside a layered medium can be retrieved from the reflection response at the surface and an estimate of the direct transmission response. In theory both the downward and upward decaying components can be retrieved. However, the retrieval of the upward decaying Green’s function is very sensitive to errors in the direct transmission response. The downward decaying

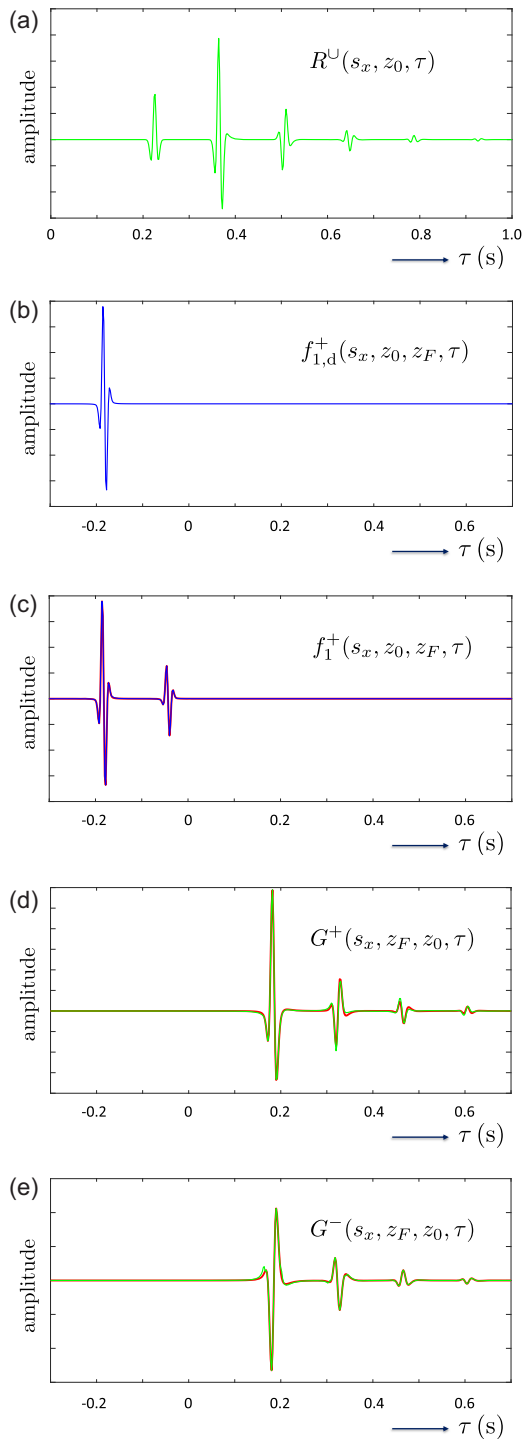


Figure 4. (a, b) Input data. (c, d, e) Results of the Marchenko method for evanescent waves at $z_F = 420$ m.

Green's function, including multiple reflections, can be retrieved quite accurately, provided the distance over which the field decays is limited. Errors in the direct transmission response cause travelt ime errors but do not give rise to scattering artefacts.

The analysis is restricted to a horizontally layered medium and a single horizontal slowness. Of course the proposed method can be applied for a range of horizontal slownesses (for propagating and evanescent waves at one or more depth levels z_F). Combining this with an inverse transform to the space-time domain, this enables

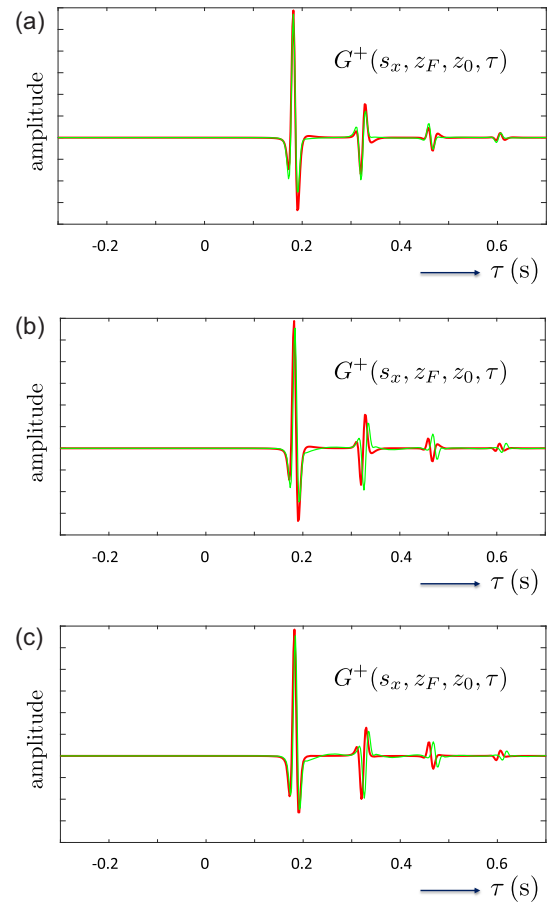


Figure 5. Results of variations of the Marchenko method for evanescent waves at $z_F = 420$ m (details discussed in the text).

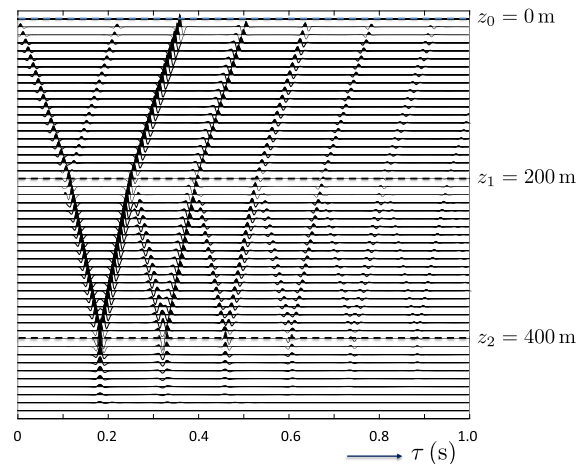


Figure 6. Results of the Marchenko method for all depth levels. To emphasize the multiples, a time-dependent amplitude gain of $\exp\{4\tau\}$ is used in this display.

the monitoring of the space-time evolution of a wave field through a layered medium, similar as in Brackenhoff *et al.* (2019) but including refracted waves. The generalisation of the proposed method for laterally varying media is subject of current research.

ACKNOWLEDGEMENTS

The constructive comments of Leon Diekmann and an anonymous reviewer are highly appreciated. This work has received funding from the European Union's Horizon 2020 research and innovation programme: H2020 European Research Council (grant agreement 742703).

REFERENCES

- Aki, K. & Richards, P.G., 1980. *Quantitative Seismology*, Vol. I, W.H. Freeman and Company.
- Brackenhoff, J., Thorbecke, J. & Wapenaar, K., 2019. Monitoring of induced distributed double-couple sources using Marchenko-based virtual receivers, *Solid Earth*, **10**, 1301–1319.
- Broggini, F. & Snieder, R., 2012. Connection of scattering principles: a visual and mathematical tour, *Eur. J. Phys.*, **33**, 593–613.
- Fokkema, J.T. & van den Berg, P.M., 1993. *Seismic Applications of Acoustic Reciprocity*, Elsevier.
- Kennett, B.L.N., Kerry, N.J. & Woodhouse, J.H., 1978. Symmetries in the reflection and transmission of elastic waves, *Geophys. J. R. astr. Soc.*, **52**, 215–230.
- Ravasi, M., Vasconcelos, I., Kritski, A., Curtis, A., da Costa Filho, C.A. & Meles, G.A., 2016. Target-oriented Marchenko imaging of a North Sea field, *Geophys. J. Int.*, **205**, 99–104.
- Rose, J.H., 2002. 'Single-sided' autofocusing of sound in layered materials, *Inverse Probl.*, **18**, 1923–1934.
- Slob, E., Wapenaar, K., Broggini, F. & Snieder, R., 2014. Seismic reflector imaging using internal multiples with Marchenko-type equations, *Geophysics*, **79**(2), S63–S76.
- Staring, M., Pereira, R., Douma, H., van der Neut, J. & Wapenaar, K., 2018. Source-receiver Marchenko redatuming on field data using an adaptive double-focusing method, *Geophysics*, **83**(6), S579–S590.
- Stoffa, P.L., 1989. *Tau-p - A Plane Wave Approach to the Analysis of Seismic Data*, Kluwer Academic Publishers.
- Ursin, B., 1983. Review of elastic and electromagnetic wave propagation in horizontally layered media, *Geophysics*, **48**, 1063–1081.
- Wapenaar, C.P.A., Peels, G.L., Budejicky, V. & Berkhout, A.J., 1989. Inverse extrapolation of primary seismic waves, *Geophysics*, **54**(7), 853–863.
- Wapenaar, K., 1998. Reciprocity properties of one-way propagators, *Geophysics*, **63**, 1795–1798.
- Wapenaar, K., Thorbecke, J., van der Neut, J., Broggini, F., Slob, E. & Snieder, R., 2014. Marchenko imaging, *Geophysics*, **79**(3), WA39–WA57.